

## FUNCTION OF VOLTAGE-GATED IONIC CHANNELS

**Mahmut OZER<sup>1</sup>**

**Abdullah BAL<sup>2</sup>**

<sup>1</sup>Zonguldak Karaelmas University, Engineering Faculty, Department of Electrical and Electronics Engineering, 67100 Zonguldak, Turkey

<sup>2</sup>Yıldız Technical University, Electrical and Electronics Engineering Faculty, 80750 Besiktas, Istanbul, Turkey

<sup>1</sup>E-mail: [mahmutozer2002@yahoo.com](mailto:mahmutozer2002@yahoo.com)

<sup>2</sup>E-mail: [bal@yildiz.edu.tr](mailto:bal@yildiz.edu.tr)

### **ABSTRACT**

*In this paper, we investigate dynamics of voltage-gated ionic channels which are of great importance in integrating the information received by neurons. Understanding of dynamical behavior of voltage-gated ionic channels plays a major role for determining underlying mechanism of spike activity and predicting the neuronal behavior. Investigation is carried out based on Hodgkin-Huxley (H-H) mathematical formalism. Ionic channel gate model is discussed briefly. Relaxation phenomenon is studied in the gate variables. Then effects of temperature on dynamics of gate variables are examined. Finally voltage-clamped simulations are carried out to determine their dynamic behaviors based on squid giant axon.*

**Keywords:** *Voltage-gated Ionic Channel, Hodgkin-Huxley, Dynamics, Squid Giant Axon*

### **1. INTRODUCTION**

Ionic channels are of great importance in the transfer of ions between the outer and the inner surface of cell membranes. Voltage-gated ionic channels that form an important class of such channels are involved in the generation and propagation of electrical signals in the excitable cell membranes. Their mathematical description plays a key role on understanding of the action potentials. In this context methods of modern neurobiology have been significantly influenced by Hodgkin and Huxley. They derived mathematical equations that describe two types of voltage-gated ionic channels in squid giant axon [1]. Neuroscientists have usually used Hodgkin-Huxley (H-H) model of coupled four-dimensional nonlinear differential equations for modeling of other neuronal structure [2]. Their

mathematical model have been particularly useful in clarifying the time-dependent behavior of nerve excitation [3]. Therefore Hodgkin-Huxley's mathematical formalism is still used to describe dynamics of voltage-gated ionic channels [4-7]. Although Clay [8] proposed an improved model for the membrane potential of the squid giant axon, it remains as a paradigm for conductance based model of neurons.

Varied properties of dynamics of the H-H model have been extensively studied in terms of their biological implications. Holden and Yoda [9] showed that the specific channel density can act as a bifurcation parameter and can control the excitability and autorhythmicity of excitable membranes by using H-H model. They also investigated the effect of channel density on the stability of the membrane potential and the

*Received Date : 06.05.2002*

*Accepted Date: 30.12.2003*

response to applied currents using numerical solutions of H-H equations [10]. Rinzel and Miller [11] argued that the conventional approach in which it's accepted that the qualitative properties of H-H model can be reduced to a two dimensional flow such as the Fitzhugh-Nagumo model is not always the case. Aihara and Matsumoto [12] examined numerical solution of H-H equations for the intact squid axon bathed in potassium-rich sea water with an externally applied inward current and showed that the equations have a complex bifurcation structure including, in addition to stable steady-states, a stable limit cycle, two unstable equilibrium points, and one asymptotically stable equilibrium point. Laboriau [13] studied H-H model in terms of the Hopf bifurcation which is critical in locating regions of bistability. Ozer [14] analyzed the axonal response of squid giant axon to sinusoidal stimulation and showed that the sinusoidal stimulus with a higher frequency results in the potential oscillation with a smaller magnitude.

On the other hand, many attempts have been carried out to examine structure and function of the voltage-gated ionic channels which are integral membrane proteins. Salman et al. [15] studied experimentally the noise in ensembles of voltage-gated ionic channels, and explained that the coupling between the microscopic state of the channels and macroscopic voltage fluctuations leads to collective effects inducing damped oscillations in the voltage noise in the context of a simple model. Following the cloning of voltage-gated ionic channels the combination of molecular biological and electrophysiological techniques has been used in the investigation of the structure and function of these membrane proteins [16-20]. These studies assist in clarifying the molecular basis of the excitability of cells. Molecular dynamics studies can enable to improve the informations of how the ionic channels function at the microscopic level [21]. In a recent study a rigorous statistical mechanical equilibrium theory of ions in the membrane channels is developed incorporating the influence of the membrane potential, and considered as a first step toward a comprehensive theory of nonequilibrium transport phenomena in ionic channels [22].

## 2. An Ionic Channel Gate Model

In the H-H mathematical model, each ionic channel is assumed to have one or more independent gates. An ionic channel gate exists in just two states, closed (C) and open (O). The gate can change from one state to the other at random. The changes are stochastic events-that is to say they occur at random in time domain- and so we can describe their timing only in probabilistic terms. There is some structure or the property of the gate that is concerned with the transition between these two states, and the word *gate* is used to describe this concept [23]. Gating is the process whereby the gate is opened and closed. There may be a number of different closed and open states, so the gating processes may involve a number of different sequential or alternative transitions from one state of the gate to another. In order for the ionic channel to be open, all of its gates must be in the open state. With these assumptions, conductance of an ionic channel through a population of identical ionic channels is defined as:

$$G_X(V,t) = g_X m^p(V,t) h^q(V,t) \quad (1)$$

where  $m$  and  $h$  show voltage-dependent probability of being open state for activation and inactivation gates respectively,  $V$  is the membrane potential,  $g_x$  is maximal conductance of ionic channel when all of the gates were in the open state,  $p$  is the number of activation gates and  $q$  is the number of inactivation gates.

The activation and inactivation gates open and close over time in response to the membrane potential according to the first-order differential equations as follows:

$$\frac{dm}{dt} = \alpha_m(V)(1-m) - \beta_m(V)m \quad (2)$$

$$\frac{dh}{dt} = \alpha_h(V)(1-h) - \beta_h(V)h \quad (3)$$

Eqs. (2) and (3) state that the closed activation gate  $(1-m)$  and the inactivation gate  $(1-h)$  open at a rate  $\alpha_m(V)$  and  $\alpha_h(V)$  respectively; and the open activation gate  $m$  and the inactivation gate  $h$  close at a rate  $\beta_m(V)$  and  $\beta_h(V)$

respectively. The rate functions  $\alpha(V)$  and  $\beta(V)$  are dependent on the potential across the membrane. The forms of the rate functions are usually determined by using a mix of theoretical and empirical considerations [24]. Eqs. (2) and (3) may be also written as :

$$\frac{dm}{dt} = \frac{m_{\infty}(V) - m}{\tau_m(V)} \quad (4)$$

$$\frac{dh}{dt} = \frac{h_{\infty}(V) - h}{\tau_h(V)} \quad (5)$$

where  $m_{\infty}(V)$  and  $h_{\infty}(V)$  are steady-state activation and inactivation respectively since m and h will get asymptotically close to this values if the voltage is held constant for a sufficient duration;  $\tau_m(V)$  and  $\tau_h(V)$  show voltage-dependent activation and inactivation time constants so that the time course for approaching these equilibrium values is described by a simple exponential with these time constants, and may be written as:

$$m_{\infty}(V) = \frac{\alpha_m(V)}{\alpha_m(V) + \beta_m(V)} \quad ; \quad h_{\infty}(V) = \frac{\alpha_h(V)}{\alpha_h(V) + \beta_h(V)} \quad (6)$$

$$\tau_m(V) = \frac{1}{\alpha_m(V) + \beta_m(V)} \quad ; \quad \tau_h(V) = \frac{1}{\alpha_h(V) + \beta_h(V)} \quad (7)$$

### 3. The Model

Analysis is carried out based on the squid giant axon model. Squid giant axon contains a fast sodium channel and a delayed rectifier potassium channel as voltage-gated ionic channel which is described by Hodgkin-Huxley (H-H). Conductance of fast sodium channel is given by

$$G_{Na} = g_{Na} m^3 h \quad (8)$$

where  $g_{Na}$  is 120 mS/cm<sup>2</sup>. Rate functions of fast sodium channel at 6.3 °C are as follows:

$$\alpha_m(v) = \frac{0.1(40+v)}{1 - e^{-(v+40)/10}} \quad ; \quad \beta_m(v) = 0.108e^{-v/18},$$

$$\alpha_h(v) = 0.0027e^{-v/20} \quad ; \quad \beta_h(v) = \frac{1}{1 + e^{-(v+35)/10}} \quad (9)$$

Conductance of delayed rectifier potassium channel is given by

$$G_K = g_K n^4 \quad (10)$$

where  $g_K$  is 36 mS/cm<sup>2</sup>. Rate functions of delayed rectifier potassium channel at 6.3 °C are as follows:

$$\alpha_n(v) = \frac{0.01(v+55)}{1 - e^{-(v+55)/10}} \quad ; \quad \beta_n(v) = 0.055e^{-v/80} \quad (11)$$

The model has only one compartment and is represented by coupled differential equations according to the H-H model. Current balance equation is

$$C_m \frac{dV_m}{dt} + I_{ion} = I_{inject} \quad (12)$$

where  $C_m$ ,  $V_m$ ,  $I_{ion}$ ,  $I_{inject}$  represent membrane capacitance, membrane potential, sum of ionic currents, and injected current respectively. Sum of the ionic currents is given by

$$I_{ion} = \sum_k G_k (V_m - E_k) = g_{Na} m^3 h (V_m - E_{Na}) + g_K n^4 (V_m - E_K) + g_L (V_m - E_L) \quad (13)$$

where  $E_k$  is Nernst equilibrium potential which is also called as a reversal potential. The change in membrane potential is expressed as follows:

$$\frac{dV_m}{dt} = \frac{1}{C_m} [I_{inject} - I_{ion}] = \frac{I_{total}}{C_m} \quad (14)$$

Rate functions of activation and inactivation gates of fast sodium channel are plotted against the membrane potential in Figure 1-(a) and -(b). Activation and inactivation time constants of fast sodium channel are shown in Figure 1-(d). Steady-state open probabilities for the m- and h-gates of the fast sodium channel is plotted in Figure 1-(e). Rate functions of activation gate of delayed rectifier potassium channel are plotted against the membrane potential in Figure 1-(c). Delayed rectifier potassium channel do not have inactivation gates. Activation time constant of delayed rectifier potassium channel is shown in Figure 1-(d). Steady-state open probability for the n-gate of the delayed rectifier potassium channel is plotted in Figure 1-(e).

In the voltage-gated ionic channels, the open probabilities of the gates are non-linear, sigmoidal functions of membrane potentials

either rising from zero to one for activation gates or falling from one to zero for inactivation gates as seen in Figure 1-(e). In the depolarization phase, activation gates open and the channel becomes activated, however inactivation gates close and the channel becomes inactivated. In the hyperpolarization phase, activation gates close and the channel becomes de-activated, however inactivation gates open and the channel becomes de-inactivated. Therefore the voltage-gated ionic channel conducts only when it is activated and de-inactivated.

$\alpha$  functions of the activation gates increase with depolarization while  $\beta$  functions decrease. In contrary of activation gates,  $\alpha$  functions of the inactivation gates decrease with depolarization while  $\beta$  functions increase as shown in Figure 1-(a), (b) and (c). Provided  $\alpha$  functions are monotone increasing and  $\beta$  functions are monotone decreasing (or vice versa), the steady-state (equilibrium) curves will always have a sigmoid shape. The potential at which  $\alpha = \beta$  is called half-activation or half-inactivation voltage since it is the voltage at which half of the activation or inactivation gates will be open at equilibrium (that is,  $m_{\infty}=0.5$  or  $h_{\infty}=0.5$ ).

Half-activation voltages are calculated as  $-40.032$  mV and  $-53.403$  mV for fast sodium channel and delayed rectifier potassium channel respectively. Half-inactivation voltage is calculated as  $-62.344$  mV for fast sodium channel.

When the membrane potential changed, activation and inactivation gate open probabilities approach to their steady-state (equilibrium) values exponentially with their time constants. Activation time constants are faster than inactivation time constants as seen in Figure 1-(d). In general, the activation time constant is faster than inactivation time constant. Otherwise the channel would never conduct ions. Also activation time constant of fast sodium channel is faster than the activation time constant of delayed rectifier potassium channel. The shorter the time constant, faster the gate response. Time constants of the gates determine the speed of the gating response. This issue is explored in detail in the next section.

#### 4. Relaxation Curves of the Gates

In order to determine the relaxation which occurs from states far from the equilibrium, it is necessary to solve dynamic equations given in Eqs. (2) and (3). We solve these dynamic equations by using the Runge-Kutta method.

In the first step, it is determined where the activation gate variable of fast sodium channel relaxes for different values of voltage. Different activation curves against time are obtained for  $-60$ ,  $-50$ ,  $-35$ ,  $-20$  and  $10$  mV membrane potential levels with  $m(0) = 1$ . Results are shown in Figure 2. The activation gate of fast sodium channel relaxes to different values as seen in Figure 2. Relaxation values of the activation curves are the same with the steady-state activation values shown in Figure 1-(e) as  $0.09371$ ,  $0.250964$ ,  $0.627331$ ,  $0.875781$  and  $0.987840$  corresponding to  $-60$ ,  $-50$ ,  $-35$ ,  $-20$  and  $10$  mV membrane potential levels respectively.

In the second step, it is determined where the inactivation gate variable of fast sodium channel relaxes for different values of voltage. Different activation curves against time are obtained for  $-80$ ,  $-60$ ,  $-50$ , and  $-40$  mV membrane potential levels with  $h(0) = 1$ . Results are shown in Figure 3. Relaxation values of the inactivation curves are the same with the steady-state inactivation values shown in Figure 1-(e) as  $0.930639$ ,  $0.416875$ ,  $0.152763$ , and  $0.050191$  corresponding to  $-80$ ,  $-60$ ,  $-50$ , and  $-40$  mV membrane potential levels respectively.

In the third step, it is determined where the activation gate variable of delayed rectifier potassium channel relaxes for different values of voltage. Different activation curves against time are obtained for  $-60$ ,  $-50$ ,  $-35$ ,  $-20$  and  $10$  mV membrane potential levels with  $n(0) = 1$ . Results are shown in Figure 4. Relaxation values of the activation curves are the same with the steady-state activation values shown in Figure 1-(e) as  $0.396132$ ,  $0.550673$ ,  $0.729058$ ,  $0.8351$  and  $0.930026$  corresponding to  $-60$ ,  $-50$ ,  $-35$ ,  $-20$  and  $10$  mV membrane potential levels respectively.

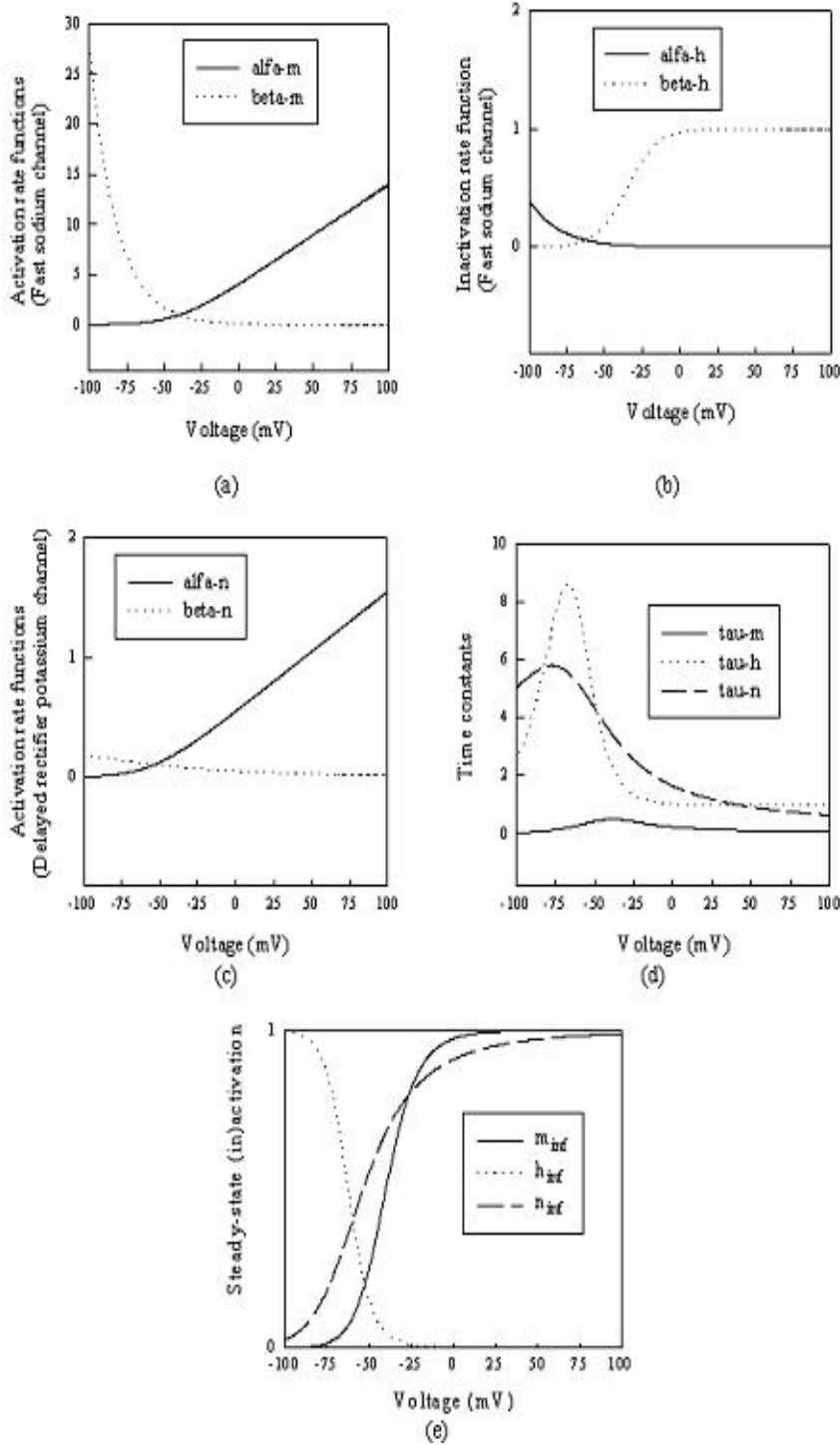


Figure 1. Activation and inactivation gate variables of ionic channels in the model

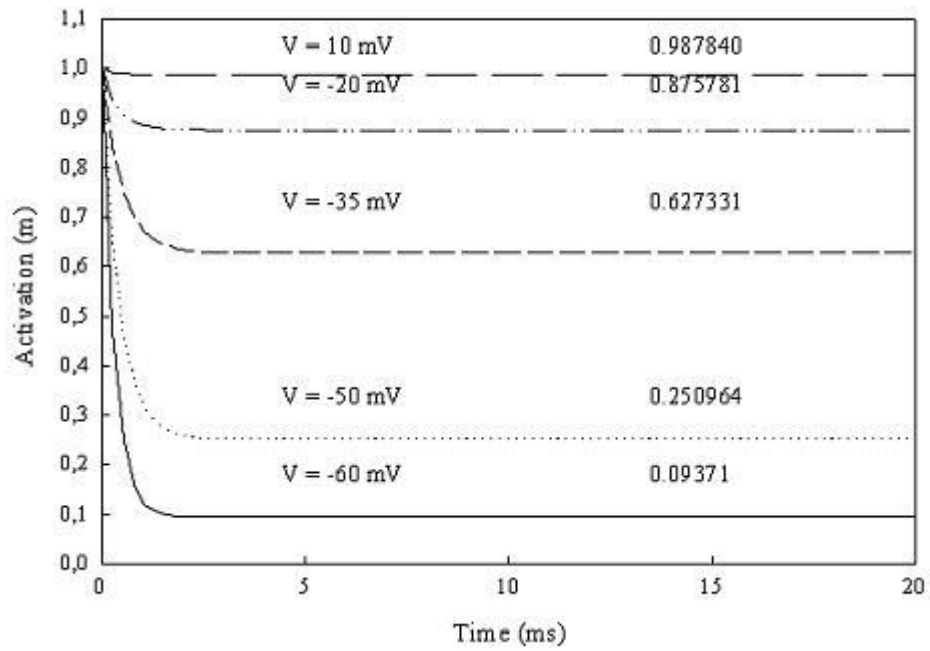


Figure 2. Fast sodium channel activation curves for different potential levels with  $m(0)=1.0$

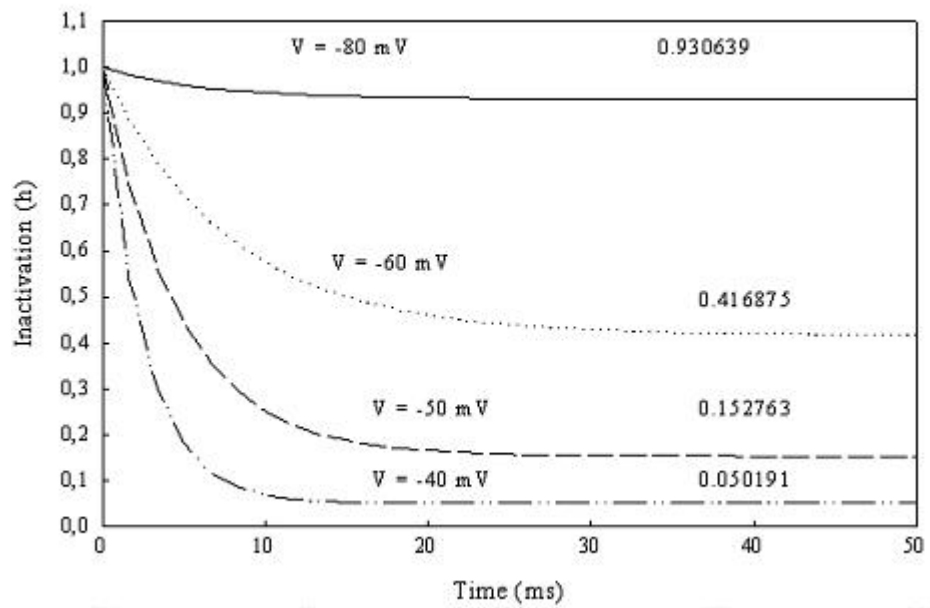


Figure 3. Fast sodium channel inactivation curves for different potential levels with  $h(0)=1.0$

Finally, the effects of initial values of the gate variables on relaxation process are investigated. For this purpose, voltage level is taken as -35 mV and different activation curves of fast sodium channel are obtained for several initial values of the activation gate variable  $m(0)$ . Obtained curves are shown in Figure 5. Activation curves relaxes to steady-state value of 0.627331 for  $V = -35$  mV faster when the initial value of the activation gate variable is nearer to its steady-state value as seen in Figure 5. Times to reach steady-state value of 0.627331 for  $V = -35$  mV are 7.2, 6.4, 6.13, 6.66 and 6.93 ms at the initial values of activation gate of 1, 0.75, 0.5, 0.25 and 0 respectively. The same properties are obtained for the inactivation gate variable of fast sodium channel and activation gate variable of delayed rectifier potassium channel, but the results are not shown here.

### 5. Effects of Temperature on Dynamics of the Gates

In this section, effects of temperature on dynamics of the gates are examined. At different temperatures far from 6.3 °C for squid

giant axon, the rate functions of the gates are multiplied by a temperature function  $\phi(T)$ . The temperature function is defined as  $\phi(T) = 3^{(T-6.3)/10}$ , where T is temperature in Celsius.

In the first step, it is determined the effects of temperature on the activation gate variable of fast sodium channel for different values of temperature. Different activation curves against time are obtained for 6.3, 7.5, 10, and 12.6 °C temperature levels with  $m(0) = 1$  and  $V = -35$  mV. Results are shown in Figure 6. The activation gate of fast sodium channel relaxes to same value with different speeds as seen in Figure 6. Activation curves relax to steady-state value of 0.627331 for  $V = -35$  mV faster when the temperature is increased. Times to reach steady-state value of 0.627331 for  $V = -35$  mV are 7.2, 6.13, 4.18, and 3.73 ms at temperature values of 6.3, 7.5, 10, and 12.6 °C respectively.

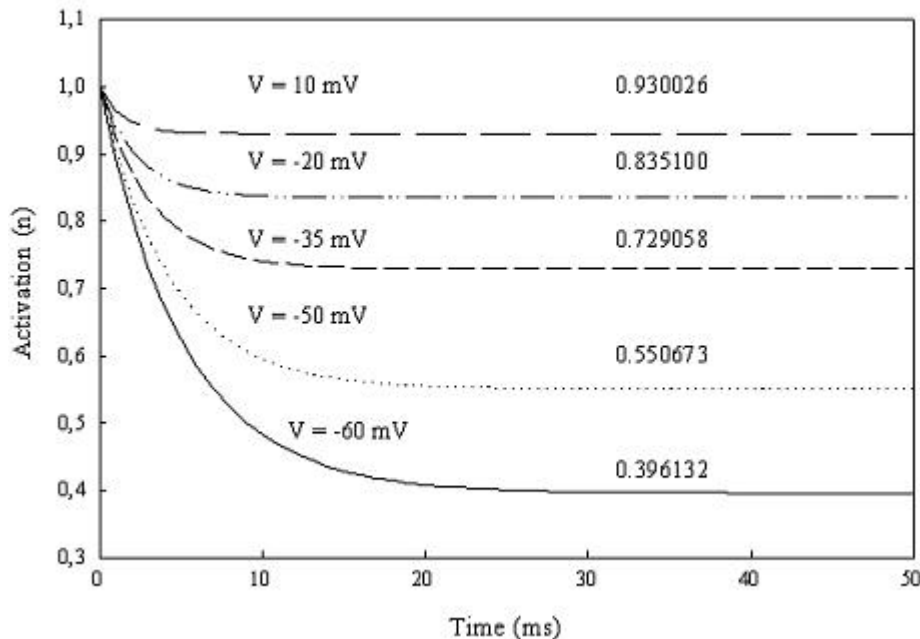
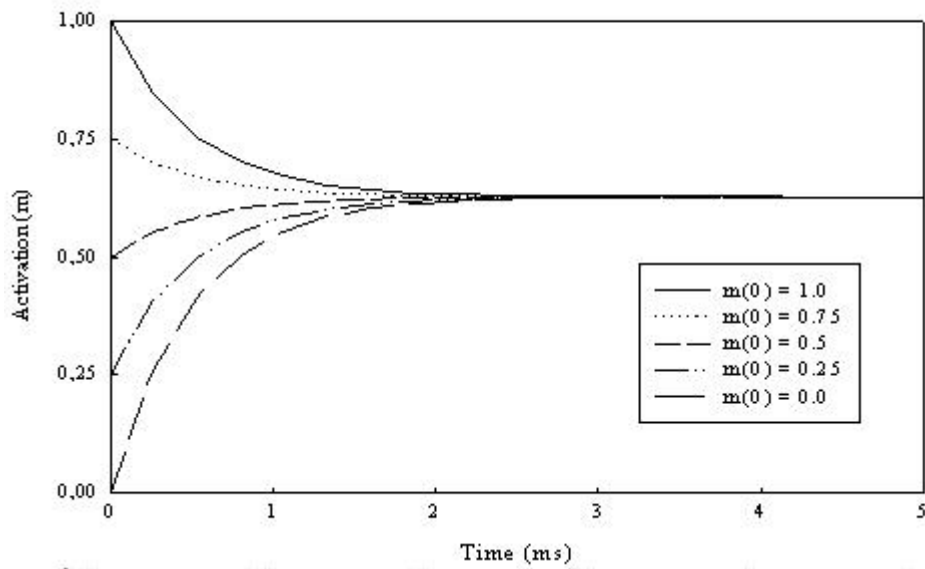
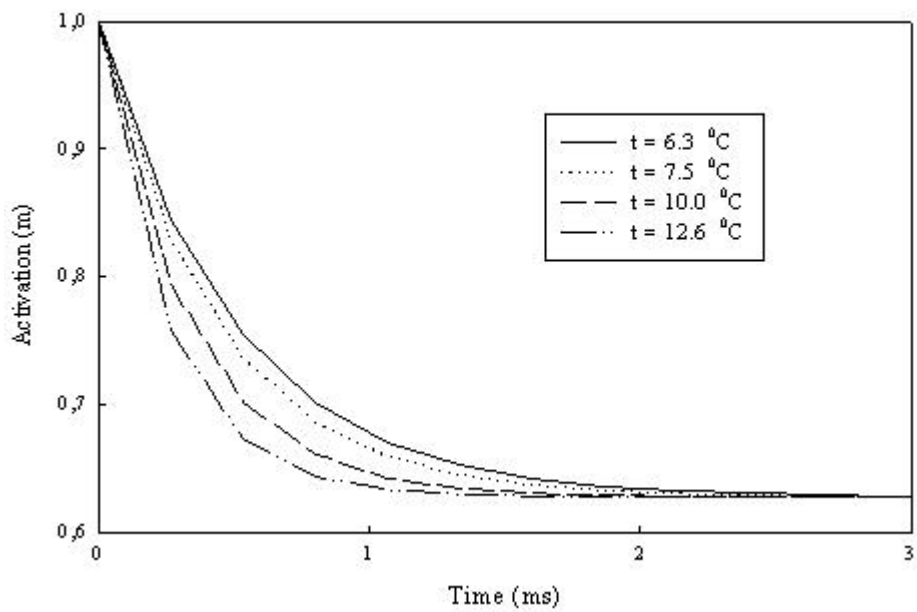


Figure 4. Delayed rectifier potassium channel activation curves for different potential levels with  $n(0)=1$



**Figure 5.** Fast sodium channel activation curves for different initial values of activation gate variable with  $V = -35$  mV



**Figure 6.** Effects of temperature on the activation gate variable of fast sodium channel with  $V = -35$  mV and  $m(0) = 1.0$



In the second step, it is determined the effects of temperature on the inactivation gate variable of fast sodium channel for different values of temperature. Different inactivation curves against time are obtained for 6.3, 7.5, 10, and 12.6 °C temperature levels with  $h(0) = 1$  and  $V = -60$  mV. Results are shown in Figure 7. The inactivation gate of fast sodium channel relaxes to same value with different speeds as seen in Figure 7. Inactivation curves relax to steady-state value of 0.416875 for  $V = -60$  mV faster when the temperature is increased. Times to reach steady-state value of 0.416875 for  $V = -60$  mV are 116.666, 101.666, 78.333, and 58.333 ms at temperature values of 6.3, 7.5, 10, and 12.6 °C respectively.

In the third step, it is determined the effects of temperature on the activation gate variable of delayed rectifier potassium channel for different values of temperature. Different activation curves against time are obtained for 6.3, 7.5, 10, and 12.6 °C temperature levels with  $n(0) = 1$

and  $V = -50$  mV. Results are shown in Figure 8. The activation gate of delayed rectifier potassium channel relaxes to same value with different speeds as seen in Figure 8. Activation curves relax to steady-state value of 0.550673 for  $V = -50$  mV faster when the temperature is increased. Times to reach steady-state value of 0.550673 for  $V = -50$  mV are 71, 62, 47, and 36 ms at temperature values of 6.3, 7.5, 10, and 12.6 °C respectively.

## 6. Voltage-clamped Simulations

Rapid membrane potential changes reflect currents through the membrane capacitance as well as movements of ions through ionic channels as seen in Eq. (12). It would be useful to study ionic currents if one gets rid of the capacitance current. The way to do this is to hold the membrane potential at a constant ('clamped') value, so that  $dV/dt = 0$ .

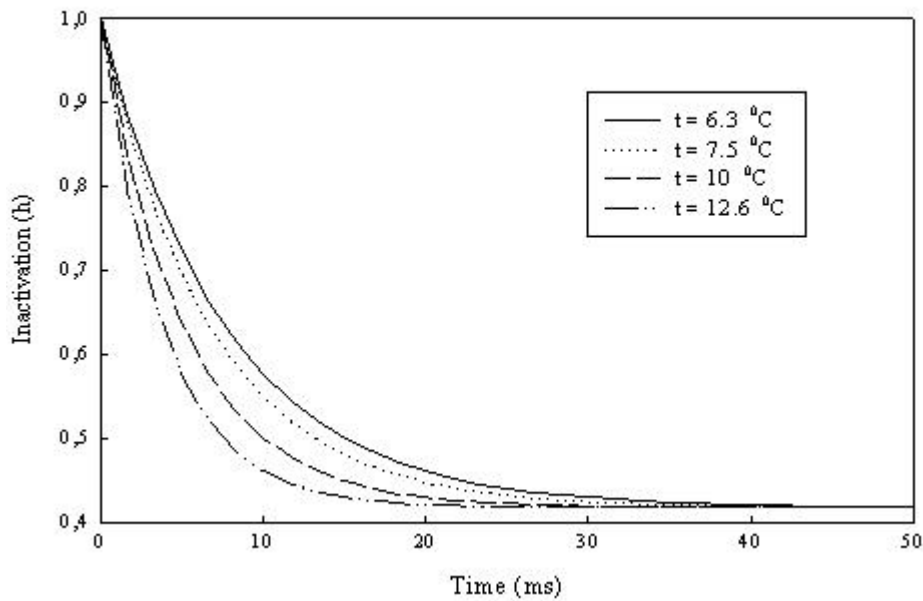


**Figure 7.** Effects of temperature on the inactivation gate variable of fast sodium channel with  $V=-60$  mV and  $h(0)=1.0$

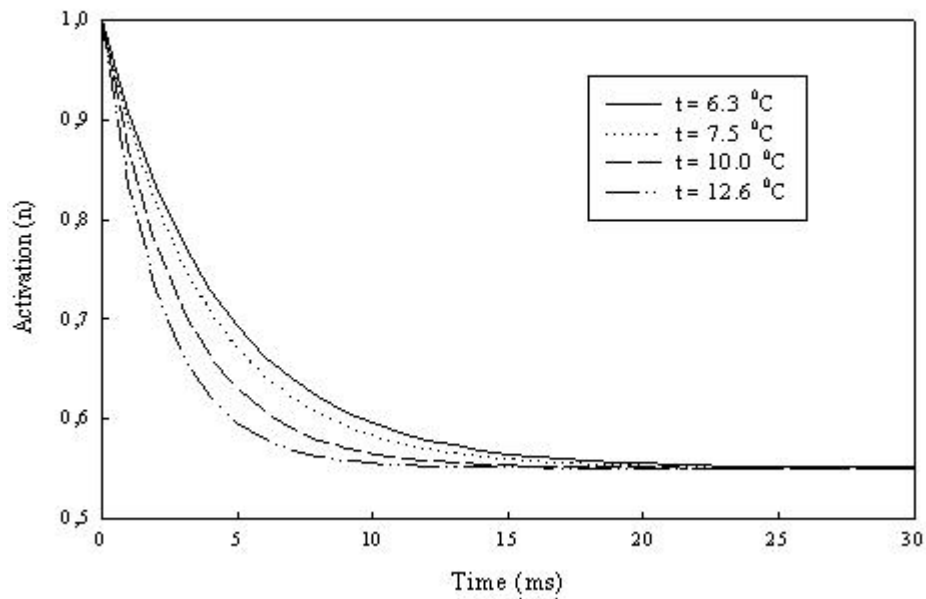


**Figure 8.** Effects of temperature on the activation gate variable of delayed rectifier potassium channel with  $V=-50$  mV and  $n(0)=1.0$

In the first step, voltage-clamped simulation is carried out for fast sodium channel. For this purpose, the membrane potential is held at a constant value of  $-70$  mV for 5 ms, then driven from  $-70$  mV to  $-20$  mV at which it is then held constant for 15 ms, then driven from  $-20$  mV to  $-60$  mV at which it is then held constant for 5 ms, and then driven from  $-60$  mV to  $-10$  mV at which it is then held constant for 10 ms, and finally driven from  $-10$  mV to  $-70$  mV at which it is then held constant for 15 ms. Obtained curves for membrane potential, open probabilities and fast sodium current are shown in Figure 9-(a), (b) and (c). Peak inward fast sodium current occurs at the maximum joint probability ( $m^3h$ ) that both the activation and inactivation gates are open as seen in Figure 9-(b) and (c). Inactivation time constant is slower or longer than the activation time constant as shown in Figure 9-(b). This enables the channel be both activated and de-inactivated at the same time for conducting.

In the second step, voltage-clamped simulation is carried out for delayed rectifier potassium channel. For this purpose, the membrane potential is held at a constant value of  $-70$  mV for 5 ms, then driven from  $-70$  mV to  $-20$  mV at

which it is then held constant for 15 ms, then driven from  $-20$  mV to  $-60$  mV at which it is then held constant for 5 ms, and then driven from  $-60$  mV to  $-10$  mV at which it is then held constant for 10 ms, and finally driven from  $-10$  mV to  $-70$  mV at which it is then held constant for 15 ms. Obtained curves for membrane potential, open probabilities and delayed rectifier potassium current are shown in Figure 10-(a), (b) and (c). Outward delayed rectifier potassium current follows the joint probability ( $n^4$ ) curve as seen in Figure 10-(b) and (c). Since delayed rectifier potassium channel does not inactivation gate, open probability for n-gate is similar to the joint probability with time delay.

## 7. CONCLUSION

Many different types of voltage-gated ionic channel are found in neurons. Voltage-gated ionic channels are of great importance in integrating the information received by the neurons. Spike activity is determined with interaction between voltage-gated ionic currents and inputs which may have synaptic or current form. Therefore understanding of dynamical behavior of voltage-gated ionic currents plays a major role for determining underlying

mechanism of the spike activity and predicting the neuronal behavior.

In this paper, dynamics of voltage-gated ionic channels is examined based on the model of squid giant axon given by Hodgkin and Huxley. Ionic channel gate model is discussed briefly.

Relaxation phenomenon is studied in the gate variables in detail. Then effects of temperature on dynamics of gate variables are examined. Finally voltage-clamped simulations are carried out to determine their dynamic behaviors based on squid giant axon.

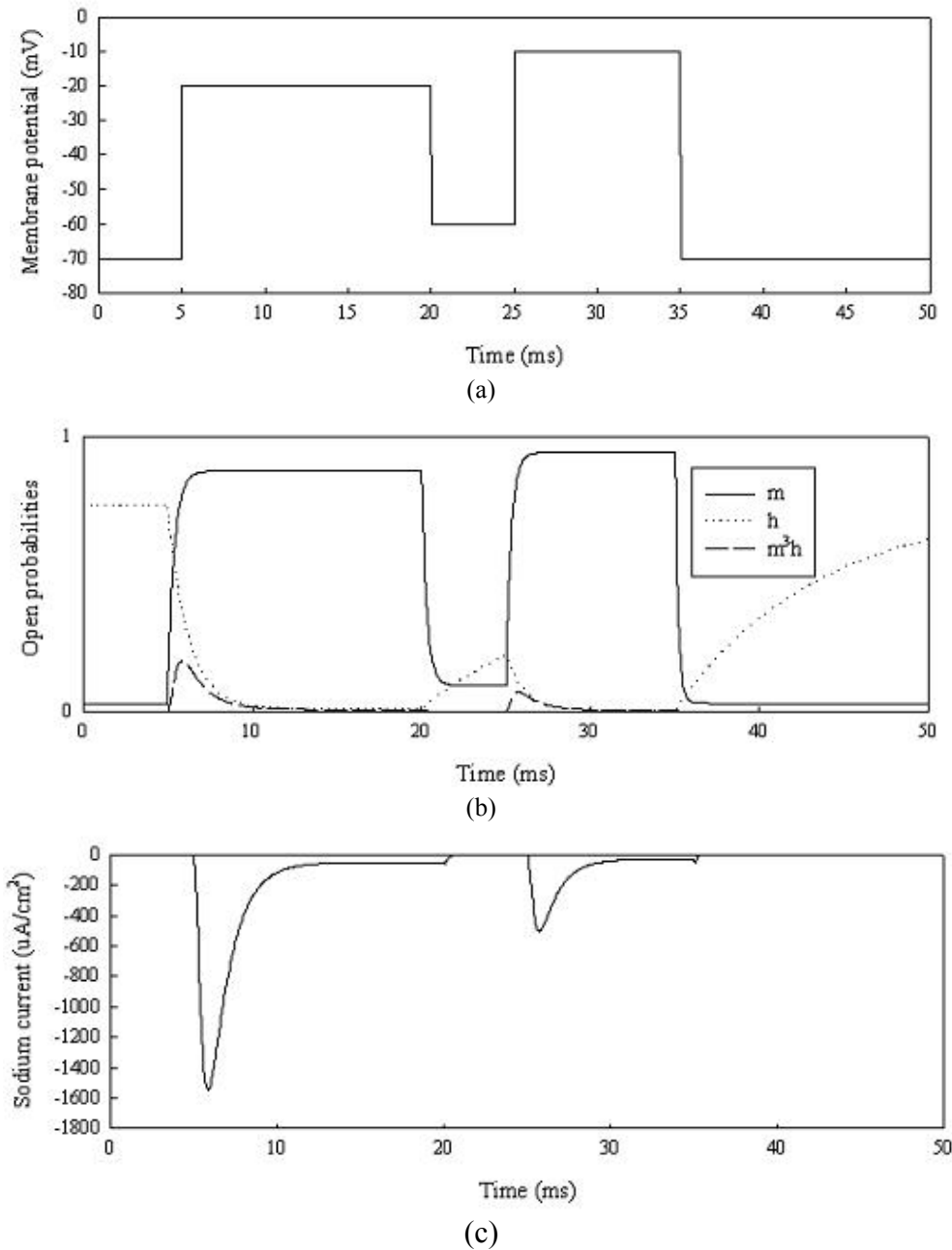


**Figure 9.** Voltage-clamped simulation for fast sodium channel: (a) clamped-voltage, (b) open probabilities and (c) fast sodium inward current

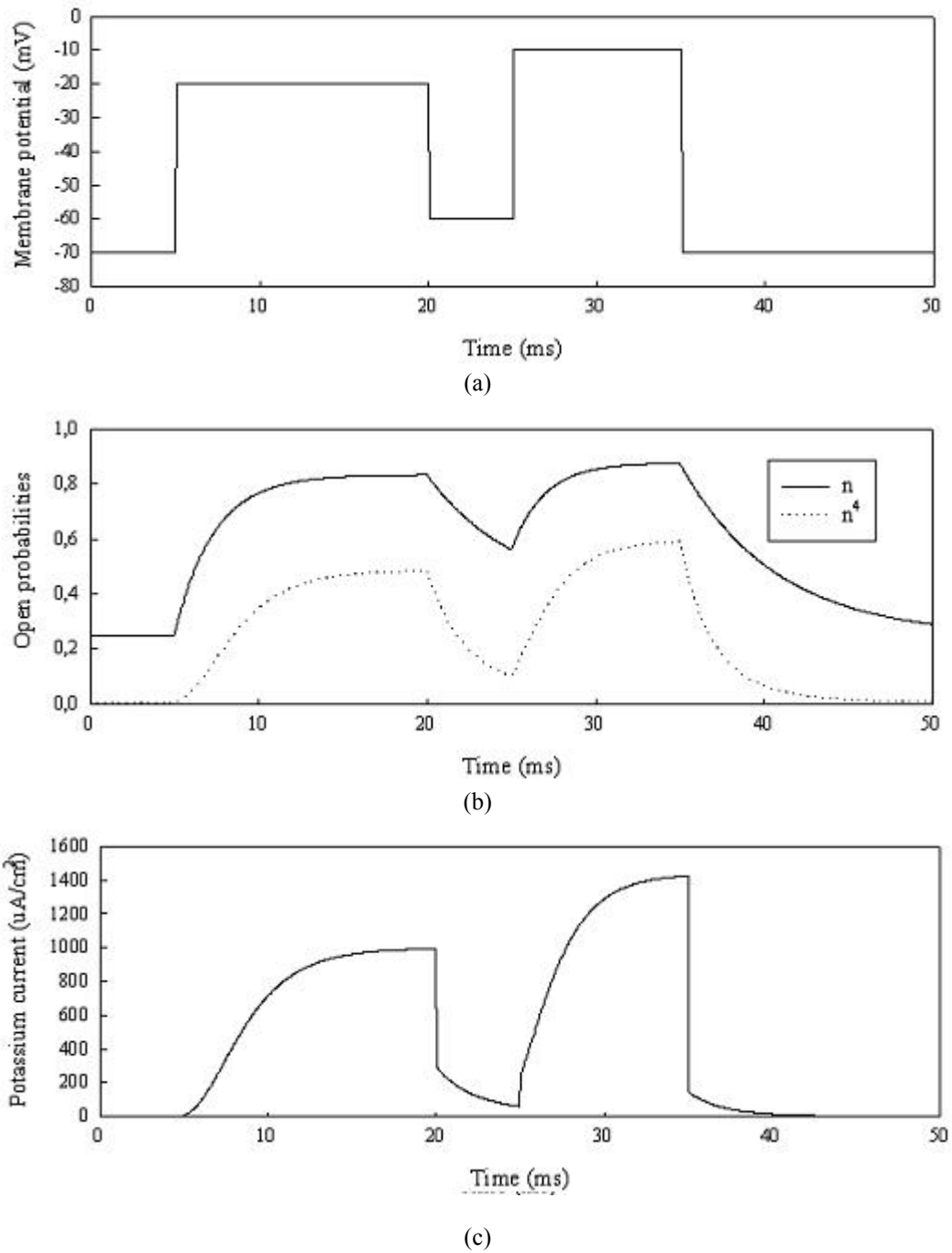


**Figure 10.** Voltage-clamped simulation for delayed rectifier potassium channel: (a) clamped-voltage, (b) open probabilities and (c) delayed rectifier potassium outward current

## REFERENCES

- [1] Hodgkin, A. L., Huxley, A. F., "A quantitative description of membrane conductance and its application to conductance and its application to conduction and excitation in nerve", *J. Physiol. (Lond.)*, Vol:117, pp.500-544, 1952.
- [2] Guckenheimer, J., Labouriau, I. S., "Bifurcation of the Hodgkin and Huxley equations: A new twists", *Bull. Math. Biol.*, Vol:55, No:5, pp. 937-952, 1993.
- [3] Aihara, K., Matsumoto, G., "Temporally coherent organization and instabilities in squid giant axons", *J. Theor. Biol.*, Vol: 95, pp. 697-720, 1982.
- [4] De Schutter, E., "Alternative equations for the molluscan ion currents described by Connor and Stevens", *Brain Res.*, Vol: 382, pp. 134-138, 1986.
- [5] De Schutter, E., Bower, J. M., "An active membrane model of the Purkinje cell: I. Simulation of current clamps in slice", *J. Neurophysiology*, Vol:71, pp. 375-400, 1994.
- [6] Sacchi, O., Belluzzi, O., Canella, R., Fesce, R., "A model of signal Processing at a mammalian sympathetic neurone", *J. Neurosci. Methods*, Vol: 80, pp. 171-180, 1998.
- [7] Ozer, M., "Analysis of time-course of the recovery from inactivation of ionic currents in cerebellar Purkinje cell", *Math. Comput. Appl.*, Vol:7, No:1, pp. 53-63, 2002.
- [8] Clay, J. R., "Excitability of the squid giant axon revisited", *J. Neurophysiol.*, Vol:80, pp. 903-913, 1998.
- [9] Holden, A. V., Yoda, M., "Ionic channel density of excitable membranes can act as a bifurcation parameter", *Biol. Cybern.*, Vol:42, pp. 29-38, 1981.
- [10] Holden, A. V., Yoda, M., "The effects of ionic channel density on neuronal function", *J. Theoret. Neurobiol.*, Vol:1, pp. 60-81, 1981.
- [11] Rinzel, J., Miller, R., "Numerical calculation of stable and unstable periodic solutions to the Hodgkin-Huxley equations", *Math. Biosci.*, Vol:49, pp.27-59, 1980.
- [12] Aihara, K., Matsumoto, G., "Two stable steady states in the Hodgkin-Huxley axons", *Biophys. J.*, Vol:41, pp. 87-89, 1983.
- [13] Laboriau, I. S., "Degenerate Hopf bifurcation and nerve impulse", *II. Siam J. Math. Anal.*, Vol:20, pp.1-12, 1989.
- [14] Ozer, M., "Analysis of axonal response to sinusoidal stimulation based on squid giant axon, International Conference on Electrical and Electronics Engineering ELECO'2001, pp. 342-344, Bursa, Turkey, 7-11 November 2001.
- [15] Salman, H., Soen, Y., Braun, E., "Voltage fluctuations and collective effects in ion-channel protein ensembles", *Phys. Rev. Lett.*, Vol:77, No:21, pp.4458-4461, 1996.
- [16] Stuhmer, W., "Structure and function of sodium channels", *Cell. Phys. Biochem.*, Vol:3, pp.277-282, 1993.
- [17] Catterall, W. A., "Structure and function of voltage-gated ion channels", *Trends in Neurosci.*, Vol:16, No:12, pp.500-506, 1993.
- [18] Catterall, W. A., "Structure and function of voltage-gated ion channels", *Ann. Rev. Biochem.*, Vol:64, pp.493-531, 1995.
- [19] Fontaine, B., Plassart-Schiess, E., Nicole, S., "Diseases caused by voltage-gated ion channels", *Molecular Aspects of Medicine*, Vol:18, No:6, pp.415-463, 1997.
- [20] Terlau, H., Stuhmer, W., "Structure and function of voltage-gated ion channels", *Naturwissenschaften*, Vol:85, No:9, pp.437-444, 1998.
- [21] Karplus, M., Petsko, G. A., "Molecular dynamics simulations in biology", *Nature*, Vol:347, pp.631-639, 1990.
- [22] Roux, B., "Statistical mechanical equilibrium theory of selective ion channels", *Biophys. J.*, Vol:77, No:1, pp.139-153, 1999.

- [23] Aidley, D. J., Stanfield, P. R., "Ion Channels", Cambridge University Press, pp.178-194, 1996.
- [24] Willms, A. R., Baro, D. J., Harris-Warrick, R. M., Guckenheimer, J., "An improved parameter estimation method for Hodgkin-Huxley models", J. Comput. Neurosci., Vol:6, pp.145-168, 1999.